

Cluster assimilation and collisional filtering on metal-oxide surfaces

Daniel A. Freedman and T.A. Arias

Laboratory of Atomic and Solid State Physics, Cornell University, Ithaca, NY 14853

(Dated: May 19, 2021)

We present the first *ab initio* molecular dynamics study of collisions between metal-oxide clusters and surfaces. The resulting trajectories reveal that internal degrees of freedom of the cluster play a defining role in collision outcome. The phase space of incoming internal temperature and translational energy exhibits regions where the collision process itself ensures that clusters which do not rebound from the surface assimilate seamlessly onto it upon impact. This filtering may explain some aspects of recent observations of a “fast smoothing mechanism” during pulsed laser deposition.

PACS numbers: 68.47.Jn, 71.15.Pd, 79.20.Ap, 68.55.Ac

The success of pulsed laser deposition of complex oxide films raises the fundamental question of how a disordered distribution of incoming clusters incorporates seamlessly into highly ordered crystals with complex unit cells. In pulsed laser deposition, a laser pulse impinges upon a target and ejects hot material into a plasma plume which then condenses upon a growing substrate[1]. With empirical tuning of parameters such as laser wavelength and energy density, laser pulse width and separation, partial pressure of the ambient gas, and substrate temperature, the resulting film can be made to grow smoothly and nearly defect free[2]. Little is known about what underlying fundamental processes these external parameters control. In recent years, sub-second time-resolved *in situ* x-ray measurements of growth by this process have become possible[3, 4]. These experiments suggest that incoming clusters from the plume are incorporated into the substrate on sub-millisecond time scales in a “fast smoothing mechanism” which occurs too quickly to be explained by traditional diffusional smoothing[4, 5]. The present work addresses the question of whether smoothing mechanisms exist over the time scale of the actual collisions between the clusters and the surface.

To address the existence of such collisional mechanisms, atomistic, as opposed to continuum, descriptions of growth are most appropriate. Current atomistic studies of crystal growth employ a number of methods, such as kinetic Monte Carlo[6, 7, 8], molecular dynamics based on classical interatomic potentials[9, 10, 11], combinations of the two[12, 13], accelerated molecular dynamics[14], and *ab initio* calculations of already deposited material[15, 16, 17]. However, kinetic Monte Carlo methods, by their nature, handle only diffusive events, not actual deposition dynamics. Although classical molecular dynamics can address collisions, the use of interatomic potentials raises the issue of accuracy, particularly in oxides, which generally have a number of different atomic species and complex physical chemistry. While *ab initio* studies of already deposited material give insights into metastable structures and transition states, they do not do so for the kinetic mechanisms active during collisions. To study such mechanisms, this *Letter*

presents the first *ab initio* molecular dynamics calculations of collisions between metal-oxide clusters and surfaces, with magnesium oxide selected as a simple model system.

Methods — All density-functional theory[18] calculations below employ the local density approximation[19] and use the total-energy plane-wave pseudopotential technique[20] with a 20 hartree (20 H) cutoff. The pseudopotentials include non-local corrections of the Kleinman-Bylander form[21] for the *p* and *d* channels.

We represent the MgO (001) surface with a 3×3 periodic supercell and three layers of atoms. The surface slabs are separated by 12.10 Å or 18.15 Å of vacuum for cold and hot incoming clusters, respectively. The in-plane lattice constant of the supercell (8.55 Å) corresponds to that of the relaxed bulk crystal. Finally, we integrate over the Brillouin zone for this wide band-gap insulator using a single k-point at the zone center.

For molecular dynamics, we employ the Verlet algorithm[22] using a time step of 2.04 fs. We maintain the electrons within 0.1 mH of the Born-Oppenheimer surface using preconditioned conjugate-gradients within the analytically continued functional approach[23]. These parameters conserve total energy to within 3 mH (0.3% of the collision energy) throughout. The initial condition of the slab is taken to be its fully-relaxed vacuum configuration at zero temperature, with the bottom layer fixed at bulk locations, a constraint also maintained during the molecular dynamics.

To study incorporation of clusters beyond the size of simple molecular units, we study collisions with the eight-atom ($N_{cl} \equiv 8$) cubic “magic cluster”[24]. To explore the role of internal degrees of freedom, we consider otherwise identical collisions with both “cold” and “hot” incoming clusters. We prepare the cold cluster by full relaxation in vacuum and the hot cluster by adiabatic heating (with no net momentum or angular momentum) to an internal kinetic energy of $K_{int} = 0.057$ H. This energy corresponds to an internal temperature of $T = K_{int}/(3N_{cl}k_B/2) \sim 1500$ K, well below the bulk melting temperature, both *ab initio* (3110 K[25]) and experimental (3250 K[26]). Finally, we give the incoming

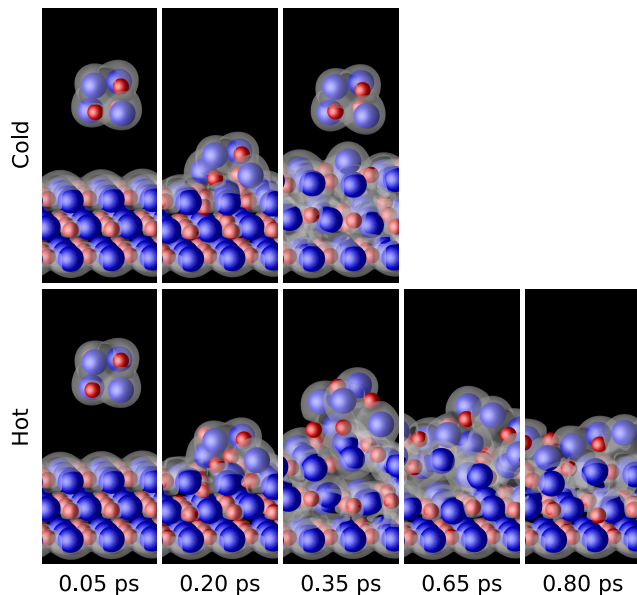


FIG. 1: (color) *Ab initio* molecular dynamics snapshots of hot and cold clusters in collision with magnesium-oxide surface: Mg cores (red), O cores (blue), electron-density isosurfaces (white), coordinate axes (upper right panel).

clusters a translational kinetic energy representative of the range (~ 10 to ~ 100 eV) which yields smooth growth in energetic deposition[1, 27]. In particular, we choose 1 H (≈ 27.21 eV), near the geometric mean of this range.

Results — Figure 1 presents snapshots of our raw results at representative times. The central result for the cold cluster (top row) is that it rebounds and does not bind to the surface. Initially ($t = 0.05$ ps), the cold cluster approaches the surface. After contact of the electron clouds, the cluster compresses while pushing atoms on the surface into the slab ($t = 0.20$ ps). The cluster then rebounds into the environment ($t = 0.35$ ps) and does not contribute to growth of the surface.

In marked contrast, the hot cluster binds to the surface. Initially ($t = 0.05$ ps), it approaches the surface with ~ 1500 K of internal kinetic energy and the same impact parameters and velocity as the cold cluster. After contact, this cluster also compresses while pushing atoms on the surface into the slab ($t = 0.20$ ps) in a configuration quite similar to that of the cold cluster. This collision dissipates sufficient translational kinetic energy for the cluster to bind to the surface ($t = 0.35$ ps). Bound, the cluster equilibrates with the surface until it assumes a rock-salt configuration conforming to the underlying crystal ($t = 0.65$ ps). Thereafter, the cluster cools until thermal vibration accounts for the remaining distortions ($t = 0.80$ ps), at which point the cluster has assimilated seamlessly onto the underlying surface.

To aid interpretation of the snapshots of the hot cluster, Figure 2 presents the internal kinetic energy (expressed as a temperature) of the hot cluster and the

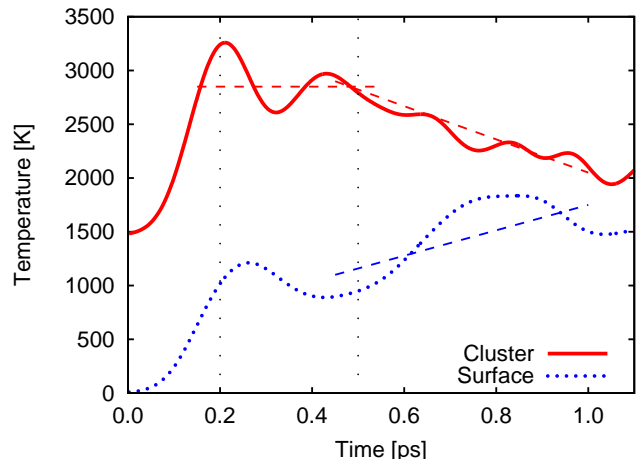


FIG. 2: (color online) Cluster (solid curve) and surface (dotted curve) temperature versus time: impacting, freezing, cooling intervals (left to right, demarked by dashed vertical lines). Dashed horizontal and diagonal lines are guides to the eye.

slab as a function of time. To reduce the appearance of fluctuations associated with the small numbers of atoms, we convolve the data with a Gaussian of width 0.05 ps. Impact occurs in the first interval indicated in the figure ($t < 0.20$ ps), during which the temperature of the slab and cluster both rise. In the following two intervals (0.20 ps $< t < 0.50$ ps; 0.50 ps $< t$), the temperature of the slab rises consistently. In contrast, the temperature of the cluster oscillates during the second interval (0.20 ps $< t < 0.50$ ps) and then drops consistently toward that of the slab during the final interval (0.50 ps $< t$). Finally, we note that a similar analysis shows that the temperature of the cold cluster also rises during the collision, but only to approximately 2000 K, well below the bulk melting point of ~ 3100 K.

Discussion — During its collision, the cold cluster never reaches the melting point and, recovering its initial form, is able to convert enough of the energy stored during the impact back into translational motion to escape the surface. In contrast, the hot cluster approaches the melting point on impact and loses its original structure. Thereafter, it cannot convert sufficient energy from the impact into translational motion to escape the surface.

Despite the small number of atoms in the cluster, thermodynamic concepts provide a useful framework for these observations. If we describe the disordering of the hot cluster as “melting,” then the translational energy which the hot cluster is unable to recover is analogous to the latent heat of fusion. We then expect the melted cluster to equilibrate with the underlying surface — first by maintaining a constant temperature while releasing the heat of fusion into the surface, and then by cooling until its temperature matches that of the surface.

The internal temperature of the hot cluster (Figure 2) arguably shows just this behavior. During the impact

in the first interval ($t < 0.20$ ps), the internal energy of the hot cluster rises to approach the bulk melting point (3100 K). In the second, “freezing,” interval (0.20 ps $< t < 0.50$ ps), the temperature shows fluctuations around a relatively constant value (horizontal dashed line in Figure 2). Consistent with this, the snapshot from the center of this interval ($t = 0.35$ ps) shows a cluster in the midst of changing its topology to conform to the underlying surface. In the third interval (0.50 ps $< t$), the cluster cools while the surface heats as the two equilibrate to a common temperature. Snapshots from this interval ($t = 0.65$ ps and $t = 0.80$ ps) show the cluster assimilated into the surface, with only thermal vibrational motion remaining.

Within the preceding framework, we make the following predictions. First, the temperature of a cluster which ensures melting upon impact should decrease with increasing incoming translational energy. There thus should be a *melting curve* in the phase space of incoming cluster temperature versus incoming translational energy, above which the cluster melts upon impact. This curve has a horizontal asymptote at the melting temperature of the cluster for low translational energies, with a horizontal intercept where the translational energy alone is sufficient to melt the cluster. Second, the cluster temperature which ensures binding after impact should increase with increasing translational energy because internal temperature promotes absorption of mechanical energy. There thus should be a *binding curve* in the phase space above which the cluster binds. This curve has a horizontal intercept at the incoming energy below which the attraction between cluster and surface always suffices to bind the cluster, followed by a vertical asymptote at the translational energy above which the cluster never absorbs sufficient energy to allow binding. Due to the ratio of bulk to surface bonds in the cluster, the translational energy above which the cluster always melts should be greater than the energy below which it always binds, so that, in general, the melting and binding curves cross. Finally, we expect that collisions will begin to disrupt the topology of the surface for translational energies somewhere near the point where there is enough energy to melt cold clusters upon impact, thus defining a *disruption curve*.

Figure 3 shows this phase space. In particular, Figure 3(a) illustrates a *melting curve*, *binding curve* and *disruption curve*, and indicates points corresponding to the above *ab initio* molecular dynamics calculations. (The specific placement of the curves and background coloring derive from classical molecular dynamics simulations described below.) The melting and binding curves define four regions in the phase space: *assimilation*, *reflection*, *tumultuation*, and *sedimentation*. In the region above both curves, clusters bind and melt and subsequently deform and *assimilate* seamlessly onto the surface upon impact. In the region below both curves, clusters neither bind nor melt and thus *reflect* intact from the surface.

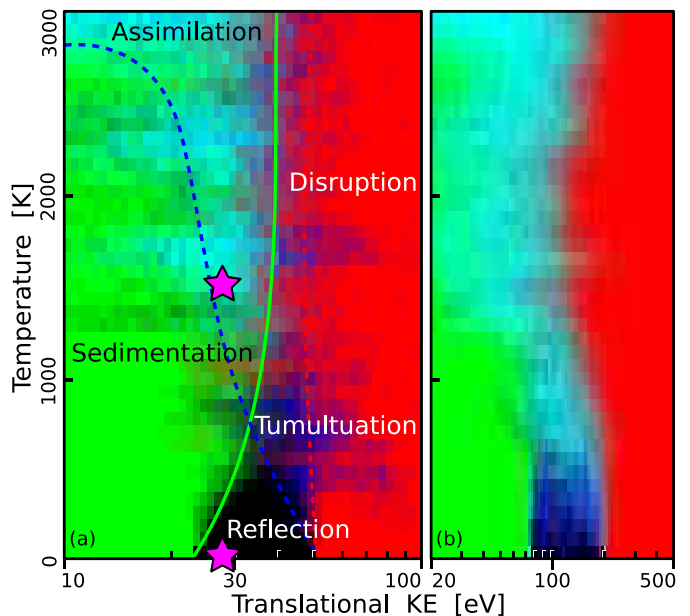


FIG. 3: (color) Phase space of incoming temperature versus translational energy for (a) small and (b) large supercells: *ab initio* results (purple stars); proposed *melting curve* (dashed blue), *binding curve* (solid green) and *disruption curve* (dotted red) overlaid on regions of *assimilation* (cyan), *reflection* (black), *tumultuation* (blue), *sedimentation* (green), and *disruption* (red), from classical molecular dynamics simulation.

In the region above the melting but below the binding curve, clusters melt but do not bind and thus *tumult* from the surface in a deformed state. In the region above the binding but below the melting curve, clusters bind but do not melt and thus *sediment* intact on the surface. Finally, the *disruption curve* defines the region where the surface topology is disrupted. The *ab initio* results conform to this demarcation of phase space, with the translational energy of 1 H such that the cold cluster (lower purple star in Figure 3(a)) reflects and the hot cluster (upper purple star in Figure 3(a)) assimilates.

To test whether these conclusions are general and insensitive to details of the underlying interactions, we construct a simple interatomic potential model of a generic divalent ionic crystal in the form of a Coulomb interaction and a pairwise short-range repulsion,

$$U = \frac{1}{2} \sum_{i \neq j} \left[\frac{q_i q_j}{r_{ij}} \left(1 - \operatorname{erfc} \frac{r_{ij}}{a_{ij}} \right) + A_0 e^{-(r_{ij}/a_{ij})^2} \right],$$

where we work in atomic units, U is the total energy of the crystal, $q_i = \pm 2$ are the ionic charges, r_{ij} is the distance between atoms i and j , $A_0 = 7$ H (fit to compromise between the lattice constant and bulk modulus of MgO) measures the strength of the repulsion between ionic cores, and a_{ij} is a range parameter defined as the mean ionic radius of atoms i and j ($R_{\text{Mg}} = 0.66$ Å, $R_{\text{O}} = 1.32$ Å). The “erfc” term is part of the short-

range repulsion between ionic cores and serves to remove the Coulomb singularity when the ionic cores overlap. This simple model material prefers rock-salt over the cesium-chloride structure, as does magnesium oxide, and has a lattice constant and bulk modulus of 5.0 Å and 240 GPa, both significantly larger (20% and 50%, respectively) than the corresponding experimental quantities for magnesium oxide.

Using the above model, we repeat the procedure of the *ab initio* molecular dynamics calculations in the same three-layer 3×3 supercell, but now map the phase space in detail: on a grid of 40 values of incoming temperature and 50 values of translational energy, sampling 25 collisions at each phase-space point, for a total of 50,000 trajectories. To explore convergence with system size, we also study a five-layer 6×6 supercell using 100,000 trajectories. Figures 3(a,b) summarize these results. The blue intensity of each pixel encodes the probability of melting; the green encodes that of binding; and the red channel encodes disruption, overriding blue and green regardless of cluster behavior. Points where clusters disrupt the surface thus appear red, whereas points where clusters assimilate appear cyan, reflect appear black, tumult appear blue, and sediment appear green. The pixelization of the figure reflects the discreteness of the sampling and the fluctuations reflect Poisson statistics ($\pm 20\%$).

Remarkably, the data in both Figures 3(a,b) correspond precisely to the expectations of the physical picture developed above. In particular, we find the expected five regions of behavior separated by the anticipated curves. Even *quantitatively*, within the corresponding supercell, the *ab initio* results fall correctly into the assimilation and reflection regions, despite the relatively small area of these regions and the quantitative differences between the *ab initio* and model materials. The larger supercell results show the same overall behavior, with quantitative correspondence for the internal temperatures and some rescaling of the translational energy. The latter effect, we believe, results from a deeper surface providing a more “cushioned” impact.

Conclusion — We present the first direct Born-Oppenheimer *ab initio* molecular dynamics calculations to demonstrate that metal-oxide clusters can assimilate seamlessly onto metal-oxide surfaces during the collisional time scale (~ 1 ps) — far shorter than diffusional time scales. These calculations, along with extensive classical molecular dynamics simulations and general physical considerations, support the novel picture that the internal degrees of freedom of the incoming clusters play an important role in deposition. The phase space of incoming temperature and translational energy summarizes important features of collision outcome, distinguishing regions of melting and binding in terms of curves whose behavior is easily understood.

The resulting phase diagram leads to new insights into pulsed laser deposition. Each laser pulse produces an en-

semble of clusters scattered across the phase space. For translational energies typical of experimental conditions for smooth growth, the arrangement of regions in the phase diagram indicates that the collision process itself provides an effective filter to ensure assimilation of clusters onto the surface *upon impact*. For translational energies above the crossing of the melting and binding curves, incoming clusters which manage to bind also melt, and thus assimilate rather than sediment. We believe that this result may relate to observations of a “fast smoothing mechanism” in growth by pulsed laser deposition[4, 5].

The authors acknowledge fruitful discussions with J. Brock, A. Fleet, and D. Dale and primary support from the NSF MRSEC program via grant DMR-9632275.

-
- [1] P. Willmott and J. Huber, *Rev. Mod. Phys.* **72**, 315 (2000).
 - [2] D. B. Chrisey and G. K. Hubler, *Pulsed Laser Deposition of Thin Films* (John Wiley, New York, 1994).
 - [3] G. Eres *et al.*, *App. Phys. Lett.* **80**, 3379 (2002).
 - [4] A. Fleet, D. Dale, Y. Suzuki, and J. Brock, *Phys. Rev. Lett.* **94**, 036102 (2005).
 - [5] P. Willmott *et al.*, *Phys. Rev. Lett.* **96**, 176102 (2006).
 - [6] E. Kotomin *et al.*, *Sol. State Comm.* **125**, 463 (2003).
 - [7] P.-M. Lam, S. Liu, and C. Woo, *Phys. Rev. B* **66**, 045408 (2002).
 - [8] O. Malis *et al.*, *Phys. Rev. B* **66**, 035408 (2002).
 - [9] X. Zhou, D. Murdick, B. Gillespie, and H. Wadley, *Phys. Rev. B* **73**, 045337 (2006).
 - [10] A. Aguado and P. A. Madden, *Phys. Rev. B* **70**, 245103 (2004).
 - [11] M. Kubo *et al.*, *J. Chem. Phys.* **107**, 4416 (1997).
 - [12] J. Jacobsen, B. Cooper, and J. P. Sethna, *Phys. Rev. B* **58**, 15847 (1998).
 - [13] J. M. Pomeroy *et al.*, *Phys. Rev. B* **66**, 235412 (2002).
 - [14] A. F. Voter *et al.*, *Annu. Rev. Mater. Res.* **32**, 321 (2002).
 - [15] J.-Y. Raty, F. Gygi, and G. Galli, *Phys. Rev. Lett.* **95**, 096103 (2005).
 - [16] V. Musolino, A. Selloni, and R. Car, *Phys. Rev. Lett.* **83**, 3242 (1999).
 - [17] G. Barcaro, A. Fortunelli, F. Nita, and R. Ferrando, *Phys. Rev. Lett.* **95**, 246103 (2005).
 - [18] P. Hohenberg and W. Kohn, *Phys. Rev.* **136**, B864 (1964).
 - [19] W. Kohn and L. Sham, *Phys. Rev.* **140**, A1133 (1965).
 - [20] M. Payne *et al.*, *Rev. Mod. Phys.* **64**, 1045 (1992).
 - [21] L. Kleinman and D. Bylander, *Phys. Rev. Lett.* **48**, 1425 (1982).
 - [22] L. Verlet, *Phys. Rev.* **159**, 98 (1967).
 - [23] T. Arias, M. Payne, and J. Joannopoulos, *Phys. Rev. Lett.* **69**, 1077 (1992).
 - [24] E. de la Puente, A. Aguado, A. Ayuela, and J. López, *Phys. Rev. B* **56**, 7607 (1997).
 - [25] D. Alfè, *Phys. Rev. Lett.* **94**, 235701 (2005).
 - [26] C. Ronchi and M. Sheindlin, *J. App. Phys.* **90**, 3325 (2001).
 - [27] D. H. Lowndes *et al.*, *Science* **273**, 898 (1996).